Development 135, 3911-3921 (2008) doi:10.1242/dev.025080

miRNAs are essential for survival and differentiation of newborn neurons but not for expansion of neural progenitors during early neurogenesis in the mouse embryonic neocortex

Davide De Pietri Tonelli[1,*,†], Jeremy N. Pulvers[1], Christiane Haffner[1], Elizabeth P. Murchison[2], Gregory J. Hannon[2] and Wieland B. Huttner[1,†]

Neurogenesis during the development of the mammalian cerebral cortex involves a switch of neural stem and progenitor cells from proliferation to differentiation. To explore the possible role of microRNAs (miRNAs) in this process, we conditionally ablated Dicer in the developing mouse neocortex using *Emx1*-Cre, which is specifically expressed in the dorsal telencephalon as early as embryonic day (E) 9.5. Dicer ablation in neuroepithelial cells, which are the primary neural stem and progenitor cells, and in the neurons derived from them, was evident from E10.5 onwards, as ascertained by the depletion of the normally abundant miRNAs *miR-9* and *miR-124*. Dicer ablation resulted in massive hypotrophy of the postnatal cortex and death of the mice shortly after weaning. Analysis of the cytoarchitecture of the Dicer-ablated cortex revealed a marked reduction in radial thickness starting at E13.5, and defective cortical layering postnatally. Whereas the former was due to neuronal apoptosis starting at E12.5, which was the earliest detectable phenotype, the latter reflected dramatic impairment of neuronal differentiation. Remarkably, the primary target cells of Dicer ablation, the neuroepithelial cells, and the neurogenic progenitors derived from them, were unaffected by miRNA depletion with regard to cell cycle progression, cell division, differentiation and viability during the early stage of neurogenesis, and only underwent apoptosis starting at E14.5. Our results support the emerging concept that progenitors are less dependent on miRNAs than their differentiated progeny, and raise interesting perspectives as to the expansion of somatic stem cells.

KEY WORDS: *Dicer* (*Dicer 1*) knockout, MicroRNAs, Neurogenesis

INTRODUCTION

The cerebral cortex, the site of higher brain function, has undergone dramatic expansion during mammalian, and notably primate, evolution (Abdel-Mannan et al., 2008; Caviness et al., 1995; Molnar et al., 2006; Rakic, 1995; Rakic, 2007). The concomitant increase in neuron number is, in essence, due to an increase in neural progenitors that undergo neurogenic divisions (Götz and Huttner, 2005; Kriegstein et al., 2006). There are two principal classes of neural progenitors that generate the neurons of the mammalian cerebral cortex: (1) the progenitors dividing at the ventricular (apical) surface of the ventricular zone (VZ) (neuroepithelial cells, radial glia and short neural precursors, collectively referred to as apical progenitors); and (2) the progenitors that divide in the basal region of the VZ and in the subventricular zone (SVZ) (referred to as basal progenitors, also called intermediate, non-surface or SVZ progenitors) (Götz and Huttner, 2005; Kriegstein et al., 2006). These distinct neural progenitors can divide to generate either progenitors, neurons, or both. The molecular machinery that regulates the balance between apical and basal progenitors, and between their neurogenic and non-neurogenic divisions, is largely unknown.

MicroRNAs (miRNAs) are a class of small RNAs that bind to specific mRNA targets, directing their degradation and/or repressing their translation (Hannon et al., 2006; Stefani and Slack, 2008). Approximately 70% of known miRNAs are expressed in the mammalian brain (Cao et al., 2006), and the level of many miRNAs changes dramatically during brain development (Krichevsky et al., 2003; Miska et al., 2004; Sempere et al., 2004). Indeed, based on observations obtained with cell culture models in vitro, miRNAs have been implicated in the control of neuronal differentiation (Conaco et al., 2006; Krichevsky et al., 2006; Makeyev et al., 2007; Smirnova et al., 2005; Wu and Belasco, 2005). Many of these investigations have focused on the in vitro role of *miR-124*, one of the most abundant miRNAs in the brain, which is highly enriched in neurons (De Pietri Tonelli et al., 2006; Hohjoh and Fukushima, 2007; Lagos-Quintana et al., 2002). These studies have revealed an important role of miRNAs in the differentiation of postmitotic neurons in vitro.

To explore a possible role of miRNAs in neuronal differentiation during the development of the mammalian nervous system in vivo, recent studies have investigated the consequences of the genetic ablation of Dicer (Dicer1 – Mouse Genome Informatics), one of the essential enzymes for the production of endogenous small interfering RNAs (siRNAs) (Watanabe et al., 2008) and for miRNA maturation (Bernstein et al., 2001; Hutvagner et al., 2001). Dicer ablation in various specific subpopulations of neurons has been found to impair neuronal differentiation and cause neurodegeneration and neuronal cell death (Cuellar et al., 2008; Davis et al., 2008; Kim et al., 2007; Schaefer et al., 2007). Although the most recent of these reports [Cuellar et al., 2008; Davis et al., 2008 (which appeared while the present study was being prepared

[1]Max-Planck Institute of Molecular Cell Biology and Genetics, Pfotenhauerstrasse 108, 01307 Dresden, Germany. [2]Cold Spring Harbor Laboratory, Watson School of Biological Sciences and Howard Hughes Medical Institute, Cold Spring Harbor, NY 11724, USA.

*Present address: The Italian Institute of Technology, via Morego 30, 16163, Genova, Italy
†Authors for correspondence (e-mails: davide.depietri@iit.it; huttner@mpi-cbg.de)

Accepted 6 October 2008

for publication)] includes the analysis of neurons in the postnatal cerebral cortex, it has remained an open issue to what extent miRNAs are essential for the early steps of neuronal differentiation that occur during embryonic development of the neocortex.

Moreover, although Dicer has been ablated in neural progenitors (Choi et al., 2008; Makeyev et al., 2007), the role of miRNAs in the progenitors that generate the neurons of the neocortex is largely unexplored, and an analysis of miRNA-dependent functions in apical versus basal progenitors and their neurogenic versus non-neurogenic divisions is lacking. Here, we have ablated Dicer in the primary neural progenitors of the neocortex, i.e. in the neuroepithelial cells of the dorsal telencephalon, and have dissected the consequences of the resulting miRNA depletion for apical and basal progenitor proliferation and differentiation, for neurogenesis, and for neuronal differentiation and survival.

MATERIALS AND METHODS

Mouse lines and genotyping

Mice were housed under standard laboratory conditions at the animal facility of the Max Planck Institute of Molecular Cell Biology and Genetics, Dresden, Germany. All experiments were performed in accordance with German animal welfare legislation (Tierschutzgesetz).

Emx1$^{Cre/wt}$ knock-in mice (Iwasato et al., 2000) were crossed with Z/EG mice (Novak et al., 2000) to obtain Z/EG^{+} *Emx1*$^{Cre/wt}$ for the analysis of Cre recombinase expression. *Dicer*$^{flox/wt}$ mice (Murchison et al., 2005) were crossed with *Emx1*$^{Cre/wt}$ knock-in mice to obtain *Dicer*$^{flox/wt}$ *Emx1*$^{Cre/wt}$ mice, and the conditional ablation of Dicer was performed by crossing the latter with *Dicer*$^{flox/flox}$ mice. The resulting *Dicer*$^{flox/wt}$ *Emx1*$^{Cre/wt}$ (control) and *Dicer*$^{flox/flox}$ *Emx1*$^{Cre/wt}$ (conditional *Dicer* knockout) littermate mice were analyzed. For *Tis21*-GFP analysis, *Dicer*$^{flox/flox}$ mice were first crossed with *Tis21*-GFP knock-in mice (Haubensak et al., 2004) to obtain *Dicer*$^{flox/flox}$ *Tis21*-GFP$^{+/+}$, which were then crossed with *Dicer*$^{flox/wt}$ *Emx1*$^{Cre/wt}$. Genotyping of mice carrying the various Z/EG, *Emx1*^{Cre}, *Dicer*^{flox} and *Tis21*-GFP alleles was performed by PCR following published protocols (Andl et al., 2006; Haubensak et al., 2004; Iwasato et al., 2000; Novak et al., 2000).

BrdU labeling

Cumulative BrdU labeling was carried out by repeated intraperitoneal injections, performed at 3-hour intervals, of pregnant females 12.5 days post-coitum (dpc) (average mouse weight, 22-24 g), using either 1 mg (4-hour time point), 800 μg (8-hour time point) or 600 μg (20-hour time point) of BrdU (Sigma-Aldrich) in PBS per injection. Mice were sacrificed 1 hour (4-hour time point) or 2 hours (8- and 20-hour time points) after the last BrdU injection, and embryos processed for analysis of BrdU-labeled nuclei in the dorsal telencephalon as described below.

For birthdating experiments, pregnant females were injected twice with 1 mg BrdU in PBS, either at 12.5 and 13.5 dpc, or at 17.5 and 18.5 dpc, and pups collected at P1 and processed for analysis of BrdU-labeled nuclei in the cortex as described below.

Immunohistochemistry and fluorescence microscopy

Immunohistochemistry and fluorescence microscopy on cryosections (10 μm) and Vibratome sections (50-70 μm) of paraformaldehyde-fixed E10.5-16.5 and P0-21 mouse brains were performed according to standard methods (Kosodo et al., 2004). Sections were incubated with primary antibodies (see below) in blocking solution for 2 hours at room temperature (cryosections) or for 24 hours at 4°C (Vibratome sections), incubated with appropriate Cy2-, Cy3- or Cy5-conjugated secondary antibodies (Jackson) in blocking solution containing 1 μg/ml DAPI (Molecular Probes) at room temperature for 1 hour (cryosections) or 2 hours (Vibratome sections), and mounted in Mowiol 4-88 (Calbiochem).

The following primary antibodies were used. Chemicon: rabbit polyclonal anti-Tbr1 and anti-BLBP, 1:500; guinea pig polyclonal anti-GLAST, 1:500. Abcam: rat monoclonal clone HTA28 anti-phosphorylated histone H3, 1:200; rabbit polyclonal anti-Foxp2, 1:500; rabbit polyclonal anti-Tbr2, 1:1000. Covance: rabbit polyclonal anti-Pax6, 1:500; mouse monoclonal anti-βIII-tubulin, 1:1000. Sigma: rabbit polyclonal anti-activated caspase 3, 1:500; mouse monoclonal anti-βIII-tubulin, 1:300. Santa Cruz: goat polyclonal anti-Brn1, 1:200. Developmental Studies Hybridoma Bank, University of Iowa, USA: mouse monoclonal clone 2H3 anti-neurofilament, 165 kDa form, 1:500. Swant: rabbit polyclonal anti-calretinin, 1:500.

For the detection of Pax6, Tbr2, Tbr1 and Brn1, cryosections prior to permeabilization were heated in 0.01 M sodium citrate at pH 6.0 in a standard microwave oven for 1 minute at 800 W, then for 10 minutes at 80 W, and allowed to cool to room temperature. BrdU detection was performed as described previously (Calegari et al., 2005). TUNEL staining was performed following the manufacturer's instructions (Roche). Nissl staining of P21 cerebral cortex Vibratome sections was performed with Cresyl-Violet acetate (Sigma) following standard protocols (Banny and Clark, 1950; Brinks et al., 2004).

Sections were analyzed by conventional (Olympus BX61) or confocal (Zeiss Axiovert 200M LSM 510) fluorescence microscopy. EGFP (Z/EG mice) and *Tis21*-GFP were detected via their intrinsic fluorescence. Images were recorded digitally and processed using Adobe Photoshop software.

Detection of miRNAs by in situ hybridization

In situ hybridization on cryosections was performed using 3′-digoxigenin-labeled LNA antisense probes (Exiqon) to mouse *miR-124* and *miR-9*, as previously described (De Pietri Tonelli et al., 2006).

Quantification and statistical analyses

Quantifications concerning the embryonic dorsal telencephalon were carried out in its lateral region, as indicated by the dashed white box in Fig. 1A, part a. Quantifications concerning the postnatal cerebral cortex were carried out in the region described in the Fig. 1 legend. Comparisons between control and Dicer-ablated animals involved littermate embryos and pups; considering the size differences between control and Dicer-ablated embryonic dorsal telencephalon and postnatal cerebral cortex that emerged during development, care was taken that corresponding regions were analyzed and that the fields compared covered the same amount of ventricular surface. Morphological measurements were performed with ImageJ version 1.33u (Wayne Rasband, National Institutes of Health, USA).

Analysis of embryonic dorsal telencephalon

For the determination of progenitor and neuronal layer thickness, the area of the neuronal layer as revealed by Tbr1 immunostaining, and that of the entire cortical wall as revealed by Tbr1 immunostaining and DAPI staining, were determined. The progenitor layer (VZ and SVZ) area was then calculated by subtracting the neuronal layer area from the entire cortical wall area. The surface of the lateral ventricle was determined in DAPI-stained sections by measuring the distance from the pallial-subpallial boundary (where the ganglionic eminence starts) to the dorsal-most point of the telencephalon (see arrowheads in Fig. 2F). Tbr2- and *Tis21*-GFP-positive nuclei in the VZ and SVZ were counted in fields, obtained with a 40× objective, the right-hand edge of which was near the pallial-subpallial boundary, and their numbers expressed as a proportion of total nuclei as revealed by DAPI staining. In similar fields, phosphohistone H3-positive cells at the ventricular surface (mitotic apical progenitors) and in the basal region of the VZ and in the SVZ (mitotic basal progenitors) were counted and their numbers expressed per field (i.e. per equal length of ventricular surface). TUNEL-positive cells were counted across the entire cortical wall and their numbers expressed per field.

Analysis of postnatal cerebral cortex

DAPI-, BrdU-, Tbr1- and Brn1-stained nuclei were counted across the entire cortical wall, except for the VZ. Numbers of Tbr1- and Brn1-positive nuclei were expressed per DAPI-stained nuclei. Numbers of Tbr1-BrdU and Brn1-BrdU double-positive nuclei, as well as nuclei stained only for BrdU, were expressed per field.

Cell cycle parameters were calculated from cumulative BrdU labeling data as previously described (Calegari et al., 2005). Statistical analysis was performed with Excel (Microsoft) using Student's *t*-test.

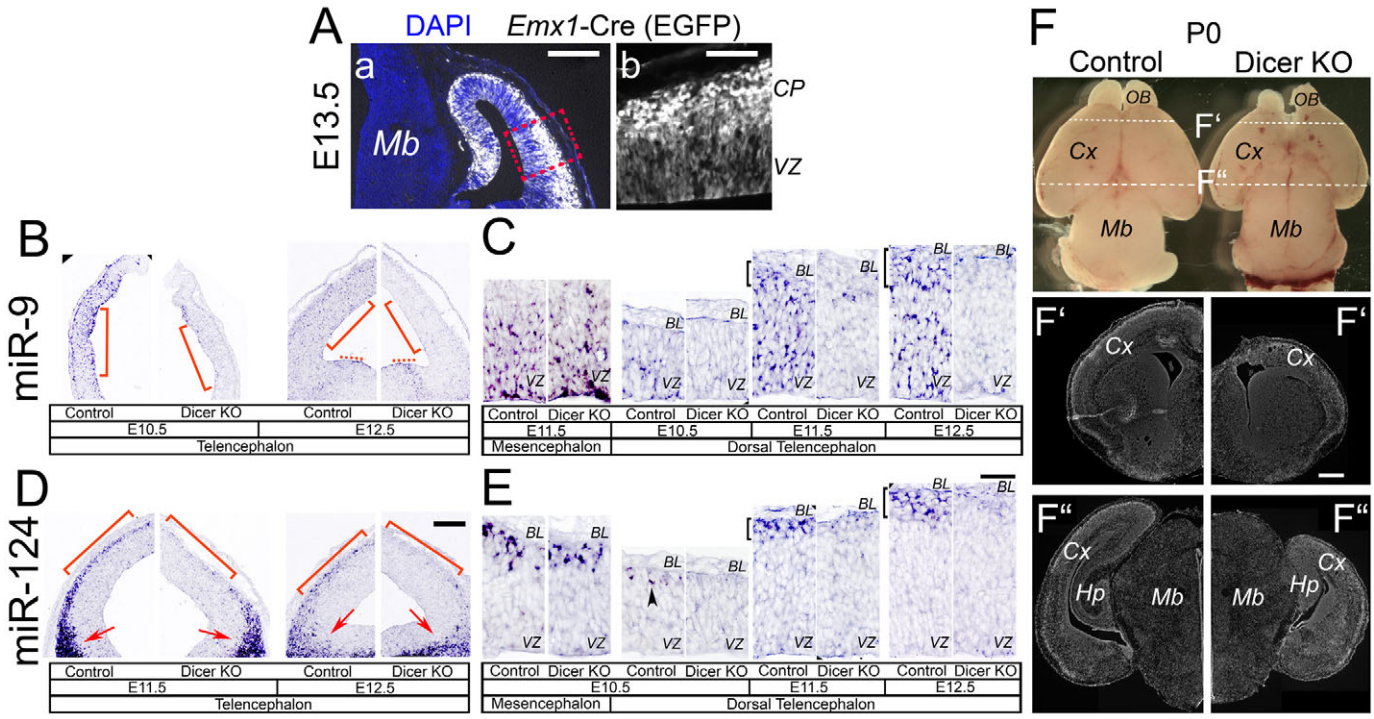

Fig. 1. Conditional ablation of Dicer in neural progenitors of the dorsal telencephalon during mouse embryonic development results in a smaller cortex. (**A**) Intrinsic EGFP fluorescence (white) with (**a**) and without (**b**) DAPI staining (blue) in a 10-μm coronal cryosection through the brain of an E13.5 mouse embryo obtained from crossing an *Emx1*$^{Cre/wt}$ mouse with a Z/EG reporter mouse. Note the specific expression of EGFP in the dorsal telecephalon. *Mb*, midbrain. The dashed box in panel a indicates the region shown at higher magnification in panel b; this region was chosen for subsequent analyses of high-magnification images (≥20× objective). (**B-E**) In situ hybridization on 10-μm cryosections through the heads of E10.5-12.5 control (*Emx1*$^{Cre/wt}$ *Dicer*$^{flox/wt}$) and conditional *Dicer* knockout (Dicer KO, *Emx1*$^{Cre/wt}$ *Dicer*$^{flox/flox}$) littermate embryos, using LNA antisense probes for *miR-9* (B,C) and *miR-124* (D,E). (B,D) Low-magnification overviews. Brackets indicate the region of the dorsal telencephalon used for subsequent analyses; dotted lines and arrows indicate the ventral telencephalon that is unaffected by *Emx1*-Cre-mediated Dicer ablation. (C,E) Higher magnification of the E10.5 (E) and E11.5 (C) mesencephalon and of the E10.5-12.5 dorsal telencephalon. Note the lack of accumulation of mature *miR-9* (B,C) and *miR-124* (D,E) specifically in the dorsal telencephalon upon Dicer ablation. *VZ*, ventricular zone; *BL*, basal lamina; brackets in C,E indicate the pre-plate (E11.5) and cortical plate (E12.5). (**F**) Comparison of P0 brains of control (*Emx1*$^{Cre/wt}$ *Dicer*$^{flox/wt}$, left) and conditional *Dicer* knockout (Dicer KO, *Emx1*$^{Cre/wt}$ *Dicer*$^{flox/flox}$, right) littermate mice. (Top) Dissected brains. Note the reduced size of the cerebral cortex (*Cx*) and olfactory bulbs (*OB*) in the Dicer KO brains. Dashed lines indicate the location of the coronal cryosections shown in F′ and F″. (**F′**,**F″**) DAPI staining of 10 μm coronal cryosections. Note the reduced size of the cortex (*Cx*) and hippocampus (*Hp*) (which lacks its typical structure), but not midbrain (*Mb*), in the Dicer KO brains. Scale bars: 500 μm in F′,F″; 250 μm in Aa,B,D; 100 μm in Ab; 50 μm in C,E.

RESULTS

Conditional ablation of Dicer in mouse cortical progenitors during embryonic development prevents miRNA maturation and results in a smaller postnatal cortex

To study the role of miRNAs in the development of the cerebral cortex, we ablated Dicer in the dorsal telencephalon in neuroepithelial cells (the primary neural stem and progenitor cells) before the onset of neurogenesis. To this end, we crossed the *Emx1*-Cre knock-in mouse line (Iwasato et al., 2000), in which Cre recombinase under the control of the *Emx1* promoter is specifically expressed in the dorsal telencephalon starting at embryonic day 9.5 (E9.5) (Simeone et al., 1992), with a mouse line carrying a conditional allele for *Dicer* (*Dicer*^{flox}), in which the essential exons 22 and 23, encoding the majority of the two ribonuclease III (RNase III) domains, are flanked by loxP sites (Murchison et al., 2005). To confirm the spatial specificity of *Emx1*-Cre-mediated recombination, we crossed the *Emx1*-Cre mice with the Z/EG reporter line (Novak et al., 2000) to reveal loxP recombination via EGFP expression. Indeed, in the developing brain at E13.5, EGFP was specifically expressed in the dorsal telencephalon (Fig. 1Aa, compare EGFP with DAPI staining) in both the primary target cells of *Emx1*-Cre-mediated recombination, the neuroepithelial cells of the VZ, and in the neurons derived from them (Fig. 1Ab). This indicated that Cre expression and, consequently, recombination, had selectively occurred in this region of the brain.

To ascertain the *Emx1*-Cre-mediated ablation of Dicer activity, we investigated whether mature miRNAs were still present in the dorsal telencephalon of *Dicer* conditional knockout embryos. For this purpose, we performed cryosection in situ hybridization using locked-nucleic-acid-modified (LNA) probes, an approach previously shown to reveal the presence of mature miRNAs but not their precursors (Kloosterman et al., 2006). As controls in these and all subsequent experiments, we used conditional heterozygous mice bearing a single *Dicer* copy (*Emx1*$^{Cre/wt}$ *Dicer*$^{flox/wt}$) in the dorsal telencephalon rather than two (*Emx1*$^{wt/wt}$ *Dicer*$^{flox/wt}$ or *Emx1*$^{wt/wt}$ *Dicer*$^{flox/flox}$), as we did not observe any obvious difference between single- and double-copy *Dicer* mice with regard to the initial parameters examined (viability, fertility, body weight, brain size), nor any obvious phenotype in the single-copy *Dicer* mice with regard to cortical development in any of the parameters analyzed.

Analysis of the E10.5-14.5 control telencephalon revealed the presence of mature *miR-9* throughout the cortical wall (Fig. 1B,C; data not shown), with the highest level in the VZ (Fig. 1C), and the presence of mature *miR-124* almost exclusively in the preplate and cortical plate (Fig. 1D,E), as previously reported (De Pietri Tonelli et al., 2006). Consistent with the *Emx1*-driven Cre-mediated recombination occurring specifically in the dorsal telencephalon (see Fig. 1A), we did observe normal levels of mature *miR-9* and *miR-124* in other brain regions, such as the mesencephalon, in both control and *Dicer* knockout littermate embryos at all stages analyzed (see Fig. 1C,E for representative examples). By contrast, upon Dicer ablation in the dorsal telencephalon, these two miRNAs were barely, if at all, detectable from E10.5 onwards (Fig. 1B-E). As *miR-9* and *miR-124* are amongst the most abundant miRNAs in the mouse brain (Hohjoh and Fukushima, 2007; Lagos-Quintana et al., 2002), our observations indicate that the conditional Dicer ablation in the dorsal telencephalon resulted in the depletion of mature miRNAs from E10.5 onwards (although persistence of low levels of some miRNAs cannot be completely excluded). Importantly, the *Emx1*-driven Cre-mediated ablation in neuroepithelial cells (Simeone et al., 1992) resulted in the depletion of mature miRNAs in both the neural progenitors themselves (as evidenced by the depletion of mature *miR-9* in the VZ) and in the neurons derived from these progenitors (as evidenced by the depletion of mature *miR-124* in the preplate and cortical plate).

To investigate the consequences of Dicer ablation during neocortical development, we first examined the postnatal cortex. At postnatal day 0 (P0), the size of the Dicer-ablated hemispheres and olfactory bulbs was clearly reduced compared with control littermate brains (Fig. 1F, top). DAPI staining of cryosections revealed, consistent with previous observations (Makeyev et al., 2007), a major reduction in the radial thickness and lateral expansion of the cortex, with the former being more evident rostrally (Fig. 1F′) than caudally (Fig. 1F″) [which perhaps reflects the gradient of *Emx1* expression (Simeone et al., 1992)]. In addition, Dicer ablation resulted in a smaller, massively disorganized hippocampus (Fig. 1F″). Consistent with the specific pattern of *Emx1*-driven Cre-mediated recombination (see Fig. 1A), the size of the midbrain was unaffected (Fig. 1F″).

At P21, the Dicer-ablated cortex was dramatically hypotrophic (see Fig. S1 in the supplementary material). Mice with Dicer-ablated cortex were viable until weaning (P21) (although their postnatal growth was markedly reduced; see Fig. S2 in the supplementary material), but died shortly thereafter (~P24-25), presumably owing to starvation and dehydration.

miRNAs are required for the proper formation of neuronal layers but not for the early development of progenitor layers

Following these observations with the postnatal cortex, we investigated the dorsal telencephalon of conditional *Dicer* knockout mice during embryonic development, distinguishing between effects on progenitors and neurons. In order to detect neurons, we performed immunofluorescence for βIII-tubulin (Tuj1; Tubb3) at E12.5, E13.5 and E14.5. At E12.5, we did not observe any obvious difference between control and conditional *Dicer* knockout embryos with respect to the thickness of the neuronal (Fig. 2A, arrowheads) or progenitor (Fig. 2A) layers as revealed by DAPI staining. By contrast, at E13.5, the Dicer-ablated cortex showed a reduced thickness of the neuronal layers (Fig. 2B, arrowheads). This phenotype was even more pronounced at E14.5, when neither a cortical plate, a subplate, nor an intermediate zone was distinguishable (Fig. 2C) (because of this disturbed cortical architecture, we use the term ‘neuronal layers’ for all layers basal to the SVZ, i.e. layers containing migrating as well as resident neurons). Remarkably, the massive reduction in the thickness of the neuronal layers at E13.5 and E14.5 upon Dicer ablation was not matched by a corresponding decrease in the progenitor layers, i.e. the VZ and SVZ (Fig. 2B,C).

To quantify these observations, we immunostained the E13.5 dorsal telencephalon for the neuron-specific transcription factor Tbr1 (Hevner et al., 2001) in order to distinguish neuronal and progenitor layers from each other and to judge the effects on neuron number versus neuronal cell volume (Fig. 2D). The thickness of the neuronal layers was found to be reduced by one-third upon Dicer ablation (Fig. 2E, white column segments), without any obvious change in nuclear density (Fig. 2D), indicating that neuron number rather than neuronal cell volume was decreased by the depletion of mature miRNAs. Consistent with the results of DAPI staining and βIII-tubulin immunofluorescence (Fig. 2B), there was no significant reduction in the thickness of the progenitor layers (Fig. 2E, black column segments).

We next compared the lateral extension of the E13.5 control and Dicer-ablated cortex. The length of the ventricular surface of the dorsolateral telencephalon was determined in consecutive DAPI-stained coronal Vibratome sections (Fig. 2F, arrowheads) and summed for an equal number of sections (12) along the rostrocaudal axis, which covered virtually all of the dorsal telencephalon for either condition. This showed that the ventricular extension of the Dicer-ablated cortex was the same as in the control.

The reduction, upon Dicer ablation, in neuron number and, consequently, in the radial thickness of the neuronal layers observed at E13.5 and E14.5 (Fig. 2) could be due to either (1) a decrease in the number of the neurons generated, (2) a loss of neurons by cell death, or (3) both. We therefore concentrated next on the process of neuron generation from progenitors.

The reduced thickness of the neuronal layer in miRNA-depleted E13.5 cortex is not due to a decrease in progenitor numbers or to alterations in progenitor lineage

Given the lack of effect on progenitor layer thickness and overall progenitor number as revealed by DAPI staining (Fig. 2), we first investigated whether Dicer ablation affected the proportion of neurogenic progenitors relative to the entire progenitor population. There are two principal classes of neural progenitors in the telencephalon: (1) the progenitors that divide at the ventricular (apical) surface of the VZ (neuroepithelial cells, radial glia and short neural precursors, collectively referred to as apical progenitors); and (2) the progenitors that divide in the basal region of the VZ and in the SVZ (referred to as basal progenitors, also called intermediate progenitors), which originate from apical progenitors (Götz and Huttner, 2005; Kriegstein et al., 2006). At E13.5, the proportion of apical progenitors that are neurogenic is relatively small (~15%), whereas the overwhelming majority of basal progenitors are neurogenic (Haubensak et al., 2004).

Apical progenitors (including the neurogenic subpopulation) can be identified by the expression of the transcription factor Pax6 (Götz and Barde, 2005), and basal progenitors by the transcription factor Tbr2 (Eomes – Mouse Genome Informatics) (Englund et al., 2005). Pax6 immunostaining of the E13.5 dorsal telencephalon revealed that the radial thickness of the VZ and its nuclear density were unaffected by Dicer ablation (Fig. 3A-D). Similarly, the distribution of basal progenitors between VZ and SVZ, as revealed by Tbr2 immunostaining (Fig. 3E,F), and their proportion relative to the total progenitor population (Fig. 3I), were unaltered.

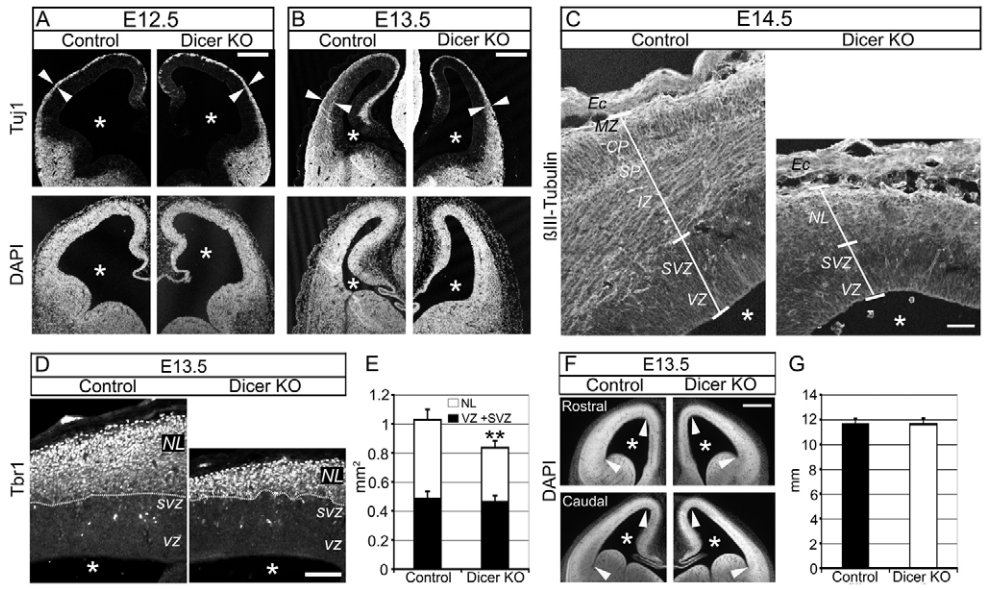

Fig. 2. Reduced thickness of the neuronal layers, but not the progenitor layers, in the Dicer-ablated E13.5 dorsal telencephalon. Comparison of the dorsal telencephalon of control (*Emx1*$^{Cre/wt}$ *Dicer*$^{flox/wt}$) and conditional *Dicer* knockout (Dicer KO, *Emx1*$^{Cre/wt}$ *Dicer*$^{flox/flox}$) littermate mouse embryos. (**A-C**) β III-tubulin (Tuj1) immunofluorescence confocal microscopy (3-μm single optical sections) of 10-μm coronal cryosections at E12.5 (A, top), E13.5 (B, top) and E14.5 (C); the E12.5 and E13.5 cryosections were co-stained with DAPI (A,B, bottom). Note the similar thickness of the neuronal layers in the control and Dicer KO cortex at E12.5 (A, arrowheads), the reduced thickness in the E13.5 Dicer KO cortex (B, arrowheads), and the absence of a recognizable structure of the neuronal layers (*NL*) in the E14.5 Dicer KO cortex (C). *IZ*, intermediate zone; *SP*, subplate; *CP*, cortical plate; *MZ*, marginal zone; *Ec*, ectoderm. (**D**) Tbr1 immunofluorescence microscopy of 10-μm coronal cryosections at E13.5. Dotted lines, basal boundary of SVZ; *NL*, neuronal layers; dashed lines, basal lamina. (**E**) Quantification of the area of the progenitor layers (VZ plus SVZ, black bars) and of the neuronal layers (NL, white bars), as indicated by the dashed white lines in D. Data are the mean of two embryos; for each embryo, the sum of the respective area of nine cryosections along the rostrocaudal axis (one field per cryosection) was calculated; bars indicate the variation of the two embryos from the mean. $^{**}P<0.01$. (**F**) DAPI staining of 70 μm coronal Vibratome-prepared sections at E13.5. The length of the ventricular surface between the two arrowheads was quantitated (see G). (**G**) Quantification of the length of the surface of the lateral ventricle. Data are the mean of two embryos; for each embryo, the sum of the length of the ventricular surface in each of 12 consecutive sections along the rostrocaudal axis was calculated; bars indicate the variation of the two embryos from the mean. Asterisks (A-C,D,F) indicate the ventricular lumen. Scale bars: 500 μm in F; 200 μm in A,B; 100 μm in D; 50 μm in C.

To specifically study the neurogenic subpopulations of apical and basal progenitors, we made use of the previously described *Tis21*-GFP (*Tis21* is also known as *Btg2* – Mouse Genome Informatics) knock-in mouse line in which these subpopulations can be identified by their nuclear GFP fluorescence (Haubensak et al., 2004). Comparison of control and Dicer-ablated mouse embryos carrying a *Tis21*-GFP knock-in allele revealed that the abundance of *Tis21*-GFP-positive (i.e. neurogenic) progenitors in the VZ and SVZ of the E13.5 dorsal telencephalon was unaltered (Fig. 3G,H,J). Taken together, these observations imply that the reduction in neuronal layer thickness at E13.5 that results from Dicer ablation in cortical progenitors was not due to a decrease in progenitor numbers, or to their switch to the neurogenic lineage.

Apical and basal progenitor cell cycle progression and divisions are unaffected by miRNA depletion until E13.5

We then investigated whether Dicer ablation affected apical and basal progenitors undergoing mitosis. Quantification of mitotic figures identified by immunostaining for phosphohistone H3 showed that the abundance of mitotic apical and basal progenitors was the same in control and Dicer-ablated E12.5 and E13.5 dorsal telencephalon (Fig. 4C,F). Also, the location of apical progenitors at the ventricular surface (Fig. 4A,B,D,E, arrows) and that of basal progenitors at the basal side of the VZ and in the forming SVZ (Fig. 4A,B,D,E, arrowheads), were indistinguishable.

To directly investigate cell cycle progression of VZ progenitors, we carried out cumulative BrdU labeling of control and Dicer-ablated E12.5 embryos in utero and quantitated the proportion of BrdU-positive nuclei in the VZ of the dorsal telencephalon after 4, 8 and 20 hours (Fig. 4J-L). For the control (Fig. 4L, black triangles), this confirmed previously reported (Calegari et al., 2005) cell cycle parameters, such as the proportion of cycling cells in the VZ (growth fraction), their cell cycle length, and the proportion of cells in S phase. In VZ progenitors of Dicer-ablated dorsal telencephalon, these cell cycle parameters were found to be very similar (Fig. 4L, white diamonds). The slightly greater proportion of BrdU-positive cells in the Dicer-ablated VZ at the three time points analyzed might not necessarily indicate a real difference to the control, but could reflect an overestimation owing, for example, to an increased presence in the VZ of neurons that were born from BrdU-positive progenitors (but did not yet express Tbr1, see Fig. 4J,K) and migrated more slowly from the VZ than in the control. Taken together, the results shown in Fig. 4A-F,J-L indicate that the cell cycle progression and division of apical and basal progenitors were unaffected by Dicer ablation until E13.5.

At E14.5 miRNA depletion decreases the abundance of mitotic apical and basal progenitors

In contrast to E12.5 and E13.5 (Fig. 4A-F), the E14.5 dorsal telencephalon showed the first clear-cut signs of Dicer ablation at the level of progenitors. Specifically, as revealed by

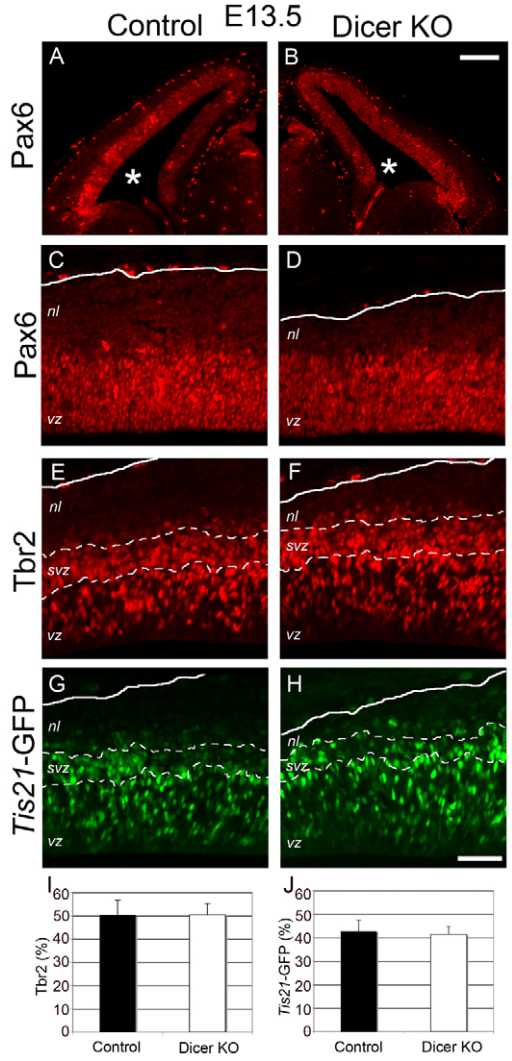

Fig. 3. Reduced thickness of neuronal layers in the Dicer-ablated E13.5 dorsal telencephalon is not due to loss of apical and basal neurogenic progenitors. (**A-H**) Immunofluorescence microscopy of 10-μm coronal cryosections through the dorsal telencephalon of control [*Emx1*$^{Cre/wt}$ *Dicer*$^{flox/wt}$ (A,C) or *Emx1*$^{Cre/wt}$ *Dicer*$^{flox/wt}$ *Tis21*-GFP$^{+/-}$ (E,G)] and conditional *Dicer* knockout [Dicer KO, *Emx1*$^{Cre/wt}$ *Dicer*$^{flox/flox}$ (B,D) or *Emx1*$^{Cre/wt}$ *Dicer*$^{flox/flox}$ *Tis21*-GFP$^{+/-}$ (F,H)] E13.5 littermate mouse embryos, showing Pax6 (A-D), Tbr2 (E,F) and *Tis21*-GFP (G,H) staining. *nl*, neuronal layers; asterisks, ventricular lumen; dashed lines, boundaries of the SVZ; solid lines, basal lamina. Scale bars: 200 μm in A,B; 50 μm in C-H. (**I**,**J**) Quantification of Tbr2-positive (I) and *Tis21*-GFP-positive (J) nuclei in the VZ plus SVZ (as indicated by the upper dashed lines in E-H), each expressed as a percentage of total, DAPI-stained nuclei (not shown). Data are the mean of 28 fields counted per condition (two embryos, seven cryosections along the rostrocaudal axis per embryo, two fields per cryosection); bars indicate s.d.

phosphohistone H3 immunostaining, the abundance of mitotic apical (Fig. 4G-I, white arrows) and basal (Fig. 4G-I, arrowheads) progenitors was significantly reduced by miRNA depletion. Concomitant with this reduction, we noticed an increased appearance of pycnotic nuclei in the VZ by DAPI staining (Fig. 4H, yellow arrows). This suggested that the reduction in mitotic progenitors was due to cell death. Interestingly, mitotic basal progenitors (Fig. 4, right-hand columns) were reduced to a greater extent than mitotic apical progenitors (Fig. 4, left columns), indicating that the former were more sensitive to the depletion of miRNAs.

miRNA depletion causes apoptosis in the cortical wall starting at E12.5

As Dicer ablation did not result in any detectable phenotype at the level of neural progenitors before E14.5, we concluded that the reduction in neuronal layer thickness observed at E13.5 (see Fig. 2) was not due to reduced neurogenesis, and therefore explored the possibility that it reflected neuronal cell death. Analysis of dorsal telencephalon by TUNEL revealed that Dicer ablation resulted in apoptosis, which was observed as early as E12.5 and increased thereafter, with a dramatic rise at E14.5 (Fig. 5). This was confirmed by immunofluorescence for activated caspase 3 (data not shown), another indicator of apoptosis. Apoptotic cells were observed throughout the cortical wall but were most frequent in the layers where neurons are born (VZ and SVZ) and in those through which newborn neurons migrate on their way to the cortical plate, and were less frequent in those layers where neurons reside (Fig. 5). In light of the lack of any reduction in apical and basal progenitors until E13.5 (see Figs 2-4), we conclude that the apoptotic cells observed throughout the Dicer-ablated cortical wall up until E13.5 were predominantly newborn neurons (that, however, lacked immunoreactivity for βIII-tubulin), suggesting that these cells were particularly sensitive to miRNA depletion.

The massive apoptosis in the Dicer-ablated VZ and SVZ at E14.5 (Fig. 5H,J) suggested that at this stage not only newborn neurons, but also progenitors, underwent apoptosis, consistent with the observed reduction in mitotic apical and basal progenitors (see Fig. 4H,I). In support of this, in the E16.5 Dicer-ablated dorsal telencephalon, we observed a dramatic reduction in the radial thickness of the progenitor layers, in BrdU incorporation, and in the expression of the radial glia markers BLBP and GLAST (Fabp7 and Slc1a3, respectively – Mouse Genome Informatics) (data not shown). Thus, concomitant with the progression of neurogenesis, neural progenitors become increasingly sensitive to miRNA depletion.

Decreased generation of upper layer neurons and lack of cortical layering in the miRNA-depleted P1 cortex

Given the loss of progenitors from E14.5 onwards, we investigated the effects of Dicer ablation on the generation of early-born neurons versus late-born neurons. For this purpose, we analyzed the P1 cortex, specifically its caudal region, in which the reduction in overall radial thickness due to Dicer ablation is less pronounced than rostrally (see Fig. 1, F′ versus F″). During mouse cortical development, early-born neurons (E12.5-13.5) form the deep cortical layers, notably layer VI, which contains strongly Tbr1-positive neurons (Hevner et al., 2001). Later-born neurons (generated between E14.5 and E18.5) accumulate in an inside-out manner above the deep layers, forming the upper layers, notably layers III and II, which contain neurons expressing the transcription factor Brn1 (Pou3f3 – Mouse Genome Informatics) (He et al., 1989). To relate the expression of the Tbr1 and Brn1 markers to the birthdate of neurons, we labeled control and Dicer-ablated embryos in utero with BrdU either at E12.5 and E13.5, when predominantly Tbr1-positive neurons and few Brn1-positive neurons are being generated (Molyneaux et al., 2007) (Fig. 6A), or at E17.5 and E18.5, when the last upper layer Brn1-positive neurons but hardly any deep layer Tbr1-positive neurons are being generated (Molyneaux et al.,

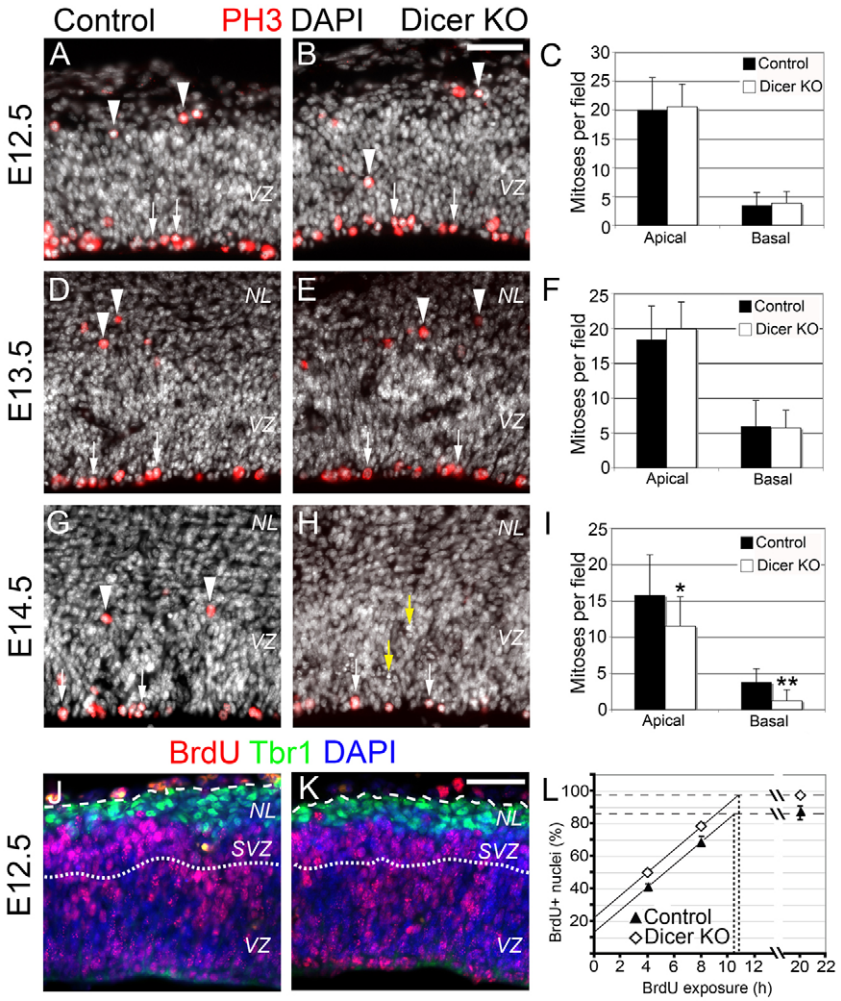

Fig. 4. The reduced thickness of neuronal layers in the Dicer-ablated E13.5 dorsal telencephalon is not due to decreased cell cycle progression or division of apical and basal progenitors. (**A**,**B**,**D**,**E**,**G**,**H**) Immunofluorescence microscopy of 10-μm coronal cryosections through the dorsal telencephalon of control (*Emx1*$^{Cre/wt}$ *Dicer*$^{flox/wt}$) and conditional *Dicer* knockout (Dicer KO, *Emx1*$^{Cre/wt}$ *Dicer*$^{flox/flox}$) E12.5 (A,B), E13.5 (D,E) and E14.5 (G,H) littermate mouse embryos, showing phosphohistone H3 (PH3, red) and DAPI (white) staining. *NL*, neuronal layers; white arrows, mitotic apical progenitors; arrowheads, mitotic basal progenitors; yellow arrows, apoptotic nuclei. (**C**,**F**,**I**) Quantification of mitotic (phosphohistone H3-positive) apical and basal progenitors at E12.5 (C), E13.5 (F) and E14.5 (I). Data are the mean of 32 (C) or 28 (F,I) fields counted per condition from two embryos, eight (C) or seven (F,I) cryosections along the rostrocaudal axis per embryo, two fields per cryosection; bars indicate s.d. *P<0.05, **P<0.01. (**J-L**) Control (*Emx1*$^{Cre/wt}$ *Dicer*$^{flox/wt}$; J,L black triangles) and conditional *Dicer* knockout (Dicer KO, *Emx1*$^{Cre/wt}$ *Dicer*$^{flox/flox}$; K,L white diamonds) E12.5 littermate embryos were subjected to cumulative BrdU labeling in utero and analyzed after 4, 8 and 20 hours. (J,K) Triple immunofluorescence microscopy of 10-μm coronal cryosections through the dorsal telencephalon after 4 hours of cumulative BrdU labeling, showing BrdU (red), Tbr1 (green) and DAPI (blue) staining. *NL*, neuronal layers. (**L**) Quantification of BrdU-positive (BrdU+), Tbr1-negative nuclei in the VZ (immunostained as in J,K), expressed as percentage of DAPI-stained nuclei. Data are the mean of two embryos; for each embryo, the average for three fields along the rostrocaudal axis (one field per cryosection) was calculated; bars indicate the variation of the two embryos from the mean (and are often smaller than the size of the symbol used). Horizontal dashed lines indicate the growth fraction. Vertical dotted lines indicate T_C–T_S (control 10.5 hours, Dicer KO 11.0 hours); T_S (length of S phase) was 2.4 hours for control and 3.4 hours for Dicer KO, and T_C (total length of the cell cycle) was 12.9 hours for control and 14.4 hours for Dicer KO. Scale bars: 50 μm.

2007) (Fig. 6D). We then analyzed the abundance and localization of the total population, as well the BrdU-labeled subpopulation, of Tbr1-positive and Brn1-positive neurons in the caudal region of the P1 cortex. This analysis yielded four major differences between the control and Dicer-ablated cortex.

First, Dicer ablation resulted in defective cortical layering. In the control (Fig. 6B,E), as expected, Tbr1-positive neurons were mostly present in layer VI and to a lesser extent also in the upper-most layers, whereas Brn1-positive neurons were mostly present in the upper layers III and II, with the progenitor layers also containing Brn1-positive cells. By contrast, in the Dicer-ablated cortex (Fig. 6C,F), both Tbr1-positive and Brn1-positive neurons appeared to be almost randomly distributed throughout the cortical wall. Second, the proportion of neurons expressing Brn1 was drastically reduced in the Dicer-ablated cortex (Fig. 6H, also compare C and F with B and E), whereas that expressing Tbr1 was slightly increased (Fig. 6G, also compare C and F with B and E). Third, when BrdU labeling had been carried out at E12.5 and E13.5 (Fig. 6A-C), the total number of BrdU-labeled nuclei and the proportion that was also Tbr1-positive in the P1 cortex were unaffected by Dicer ablation, but the proportion of Brn1-positive BrdU-labeled nuclei was strongly (~4-fold) reduced and, correspondingly, that of BrdU-labeled nuclei

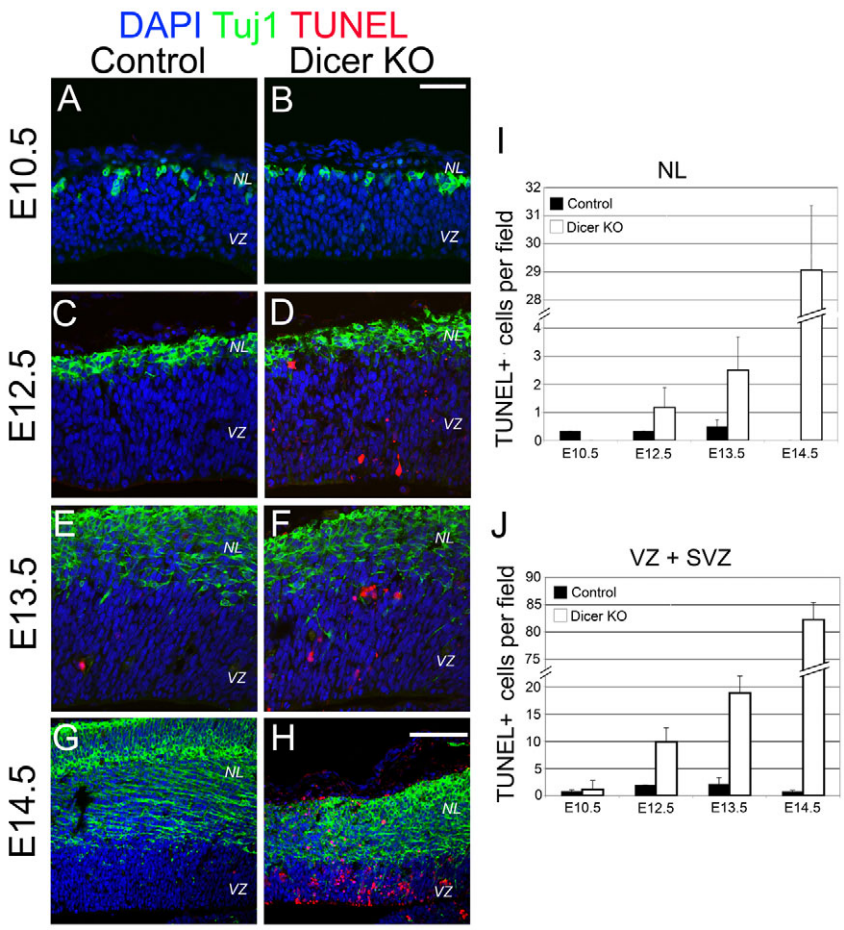

Fig. 5. Dicer ablation in the dorsal telencephalon causes progressive apoptosis starting at E12.5. (**A-H**) Immunofluorescence confocal microscopy (6-μm single optical sections) of 10-μm coronal cryosections through the dorsal telencephalon of control (*Emx1*$^{Cre/wt}$ *Dicer*$^{flox/wt}$) and conditional *Dicer* knockout (Dicer KO, *Emx1*$^{Cre/wt}$ *Dicer*$^{flox/flox}$) E10.5 (A,B), E12.5 (C,D), E13.5 (E,F) and E14.5 (G,H) littermate mouse embryos, showing βIII-tubulin (Tuj1, green), TUNEL (red) and DAPI (blue) staining. *NL*, neuronal layers. Scale bars: 50 μm. (**I**,**J**) Quantification of TUNEL-stained (TUNEL+) cells in the cortical wall. Data are the mean of two embryos; for each embryo, the average for three fields along the rostrocaudal axis (one field per cryosection) was calculated; bars indicate the variation of the two embryos from the mean. Note the interruption in the scale of the ordinate to accommodate the data for the E14.5 Dicer KO.

containing neither Tbr1 nor Brn1 massively increased (Fig. 6I). Fourth, when BrdU labeling had been carried out at E17.5 and E18.5 (Fig. 6D-F), the total number of BrdU-labeled nuclei in the Dicer-ablated P1 cortex was markedly reduced (by 60%), which was largely due to a decrease in Brn1-positive BrdU-labeled nuclei (Fig. 6J).

Considering these observations collectively, we conclude that at the early stage of cortical neurogenesis (E12.5-13.5), consistent with the lack of an overt phenotype at the progenitor level before E14.5 (Figs 2-4), neuron generation is not impaired in quantitative terms by miRNA depletion, but is affected qualitatively in that the neuronal subtype specification for the layers that are formed subsequent to the deep layers is deficient or altered. At later stages of cortical neurogenesis (from E14.5 onwards), and presumably reflecting the progressive loss of progenitors in the Dicer-ablated cortex (Fig. 4I and Fig. 5H), the generation of neurons for the upper layers is quantitatively reduced. One, although not necessarily the only, consequence of this reduced upper layer neuron production with regard to the architecture of the Dicer-ablated cortex is the relative dominance of Tbr1-positive neurons throughout the cortical wall.

miRNAs are required for proper neuronal differentiation in vivo

The deficient or altered neuronal subtype specification at the early stage of cortical neurogenesis (Fig. 6I), and the defective cortical layering as indicated by the intermixing of the few remaining Brn1-positive neurons with the Tbr1-positive neurons observed at P1 (Fig. 6C,F), raised the possibility that miRNA depletion not only decreased upper layer neuron production quantitatively, but also affected certain aspects of neuronal differentiation. The transcription factor Foxp2, which like Tbr1 is expressed by layer VI neurons, has been implicated in postmigratory neuronal differentiation (Ferland et al., 2003). We therefore examined Foxp2 expression in the control and Dicer-ablated P0 and P7 cortex. In contrast to Tbr1, which was abundantly expressed in the P1 cortex (Fig. 6), Dicer ablation almost completely abolished Foxp2 expression in the postnatal cortex (Fig. 7). This implies that miRNAs are required for proper neuronal differentiation.

Lack of interneurons and defective cortical connections in the miRNA-depleted P7 cortex

The increase in BrdU-labeled nuclei containing neither Tbr1 nor Brn1 (Fig. 6I), besides suggesting deficient or altered neuronal subtype specification, could also reflect an increased entry into the cortex of interneurons that were generated in germinal zones not affected by Dicer ablation (i.e. outside of the *Emx1* domain) (Wonders and Anderson, 2006). We investigated this issue by immunostaining the control and Dicer-ablated P7 cortex for calretinin (calbindin 2), a marker for a subset of cortical interneurons (Wonders and Anderson, 2006). This revealed a dramatic decrease, rather than an increase, in these interneurons in the Dicer-ablated cortex (see Fig. S3 in the supplementary material). Moreover, the few calretinin-positive interneurons observed were scattered throughout the cortical wall, and their neurites appeared to be poorly developed.

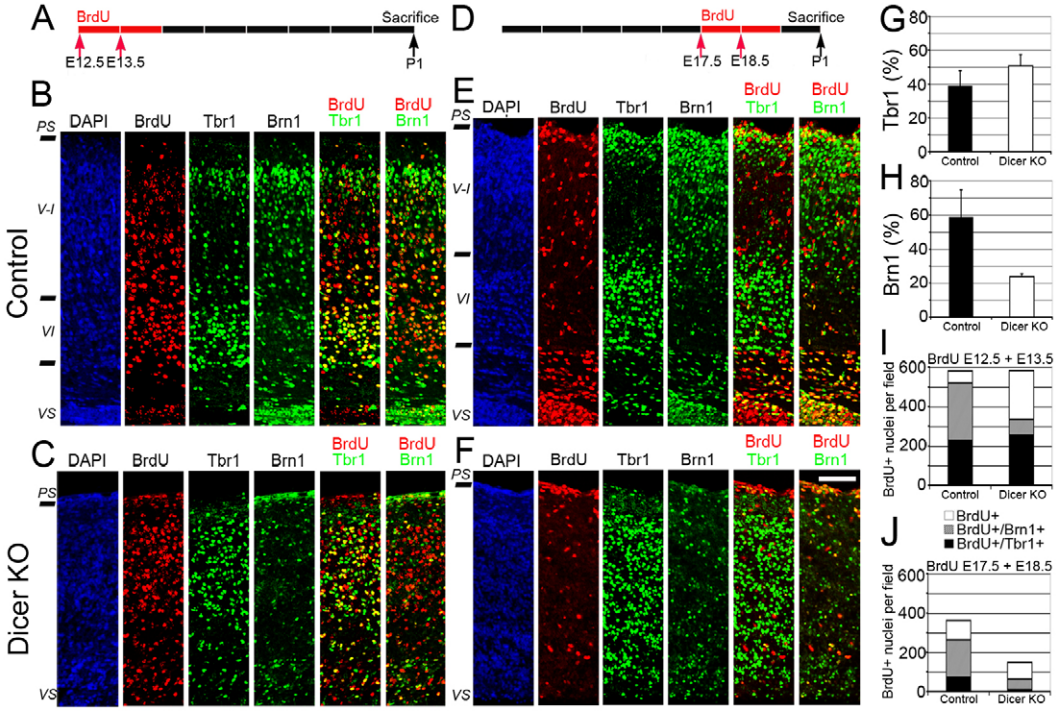

Fig. 6. Dicer ablation in the embryonic dorsal telencephalon results in reduced upper layer neurons, but not deep layer neurons, in the postnatal cortex. (**A-F**) Control (*Emx1*$^{Cre/wt}$ *Dicer*$^{flox/wt}$; B,E) and conditional *Dicer* knockout (Dicer KO, *Emx1*$^{Cre/wt}$ *Dicer*$^{flox/flox}$; C,F) mouse embryos were subjected to BrdU labeling in utero either at E12.5 plus E13.5 (B,C) or at E17.5 plus E18.5 (E,F), and the respective littermate pups were analyzed at P1, as outlined in A,D. (B,C,E,F) Triple immunofluorescence confocal microscopy (3-μm single optical sections) of 10-μm coronal cryosections through the caudal cortex stained for BrdU (red), Tbr1 (green) and Brn1 (green); DAPI staining in blue. Ventricular surface (*VS*), layers VI and V-I, and the pial surface (*PS*) are indicated on the left. Scale bar: 50 μm. (**G**,**H**) Quantification of Tbr1-positive (G) and Brn1-positive (H) nuclei (immunostained as in B,C,E,F) in the cortical wall (excluding the VZ; see the densely packed Brn1-positive layer in the control cortex at the bottom of the corresponding panel), each expressed as percentage of DAPI-stained nuclei. Data are the mean of three fields from independent experiments; one third of two of these fields is shown in B,E, and in C,F. Bars indicate s.d. (**I**,**J**) Quantification of BrdU-labeled (BrdU+) nuclei (immunostained as in B,C,E,F) in the cortical wall (defined as in G,H). Data are for the field of which one third is shown in B,C (I), and in E,F (J). BrdU-labeled nuclei were scored for immunoreactivity with Tbr1 (black), Brn1 (gray), or neither (white).

To obtain more-representative information about the formation of cortical connections, control and Dicer-ablated P7 cortex was immunostained for neurofilament protein. The miRNA-deficient cortex showed a massive reduction in, and a disorganized architecture of, cortical connections (see Fig. S3 in the supplementary material). In line with the lack of Foxp2 expression (Fig. 7), this provided further evidence that key aspects of neuronal differentiation were greatly perturbed in the miRNA-depleted cortex (Molyneaux et al., 2007; Price et al., 2006).

DISCUSSION

We have investigated the requirement for Dicer in neocortical progenitors and their progeny during mouse embryonic development. The most remarkable finding of our study is the differential sensitivity of progenitors and neurons to miRNA depletion. Dicer was ablated in neuroepithelial cells, which are the primary neural progenitors, in the dorsal telencephalon prior to the onset of neurogenesis. Yet, the cells most sensitive to the resulting miRNA depletion were neurons, followed by the committed progenitors that produce them – the basal progenitors and neurogenic radial glial cells. By contrast, neuroepithelial cells continued to proliferate normally after Dicer ablation, although their cell cycle is shorter than that of neurogenic progenitors (Calegari et al., 2005), and hence dilution of pre-existing miRNAs should have occurred earlier in the former than in the latter.

Why are neurons and neurogenic progenitors more sensitive to miRNA depletion than the stem-cell-like neural progenitors? An intriguing possibility is that when cells alter their state (e.g. from uncommitted to committed progenitor, or from cycling neurogenic progenitor to postmitotic neuron) and therefore carry out major changes in their gene expression profile, they are more dependent on miRNA-mediated regulation than when the progenitors and their progeny are very similar.

This concept is not only consistent with the general idea that ‘miRNAs confer precision and robustness to developmental processes’ (Stark et al., 2005), specifically with regard to brain development, but it is also in line with the prevailing notion (Choi et al., 2008; Conaco et al., 2006; Krichevsky et al., 2003; Krichevsky et al., 2006; Makeyev et al., 2007; Miska et al., 2004; Sempere et al., 2004; Smirnova et al., 2005; Wu and Belasco, 2005) that miRNAs are required for neuronal differentiation, for which the present study provides two further lines of evidence. One is the deficient or altered neuronal subtype specification that is suggested by the increase, upon Dicer ablation, in BrdU-labeled nuclei containing neither Tbr1 nor Brn1. The other is the lack of Foxp2 expression in layer VI neurons of the miRNA-deficient cortex. Both phenotypes are indicative of a perturbation of the gene expression changes that are normally concomitant with neuronal differentiation.

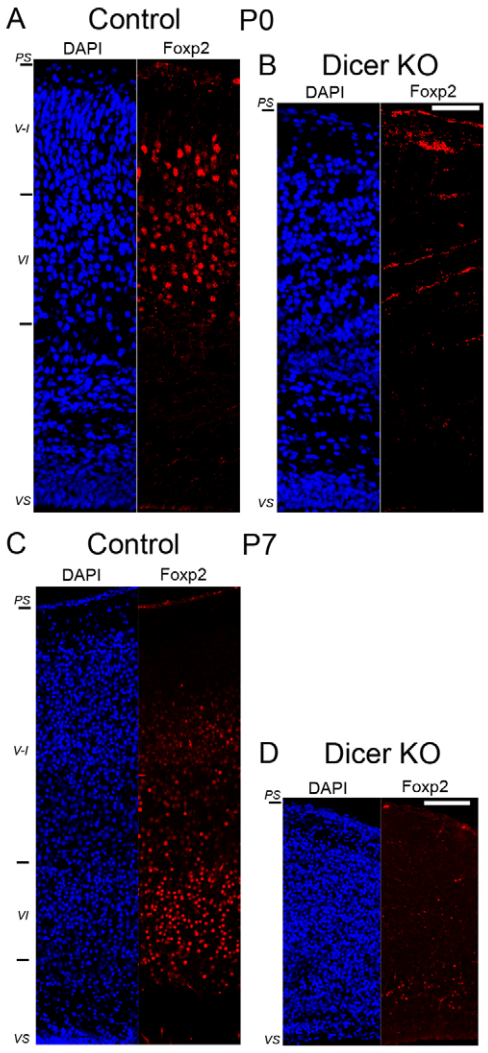

Fig. 7. Lack of Foxp2 expression in the postnatal Dicer-ablated cortex. (**A-D**) Immunofluorescence confocal microscopy of 10 μm coronal cryosections (A,B; 3-μm single optical sections) or 50 μm coronal Vibratome-produced sections (C,D; 6-μm single optical sections) through the cerebral cortex of control (*Emx1*$^{Cre/wt}$ *Dicer*$^{flox/wt}$; A,C) and conditional *Dicer* knockout (Dicer KO, *Emx1*$^{Cre/wt}$ *Dicer*$^{flox/flox}$; B,D) P0 (A,B) and P7 (C,D) littermate mice, showing DAPI (blue) and Foxp2 (red) staining. Note the almost complete absence of Foxp2-positive neurons in the cerebral cortex of P1 and P7 Dicer-ablated mice. Ventricular surface (*VS*), layers VI and V-I, and the pial surface (*PS*) are indicated on the left. Scale bars: 50 μm in A,B; 100 μm in C,D.

The idea that the proliferation of neural progenitors is less sensitive to miRNA depletion than their differentiation, together with our observation that the cell cycle progression and division of Pax6-positive apical progenitors were unaffected until E13.5, i.e. for ~8 cell cycles after the onset of Dicer ablation (Calegari et al., 2005; Simeone et al., 1992), raise interesting perspectives with regard to the expansion of neural progenitor cells. This expansion is typically curtailed as a consequence of the progeny derived from the initial progenitor population becoming increasingly differentiated. Our observations imply that the physiological expansion of Pax6-positive apical progenitors proceeds normally upon depletion of miRNAs. Perhaps, interfering with the miRNA-mediated regulation of the changes in gene expression that accompany differentiation will increase our repertoire of approaches to achieve expansion of neural progenitors, and possibly of mammalian somatic stem cells in general. Consistent with this proposal, a recent study has shown that germline stem cell maintenance in the *Drosophila* ovary is not impaired by the absence of miRNAs (Shcherbata et al., 2007).

We thank Dr Takuji Iwasato and Prof. Shigeyoshi Itohara, RIKEN institute, Wako, Japan, for kindly providing the *Emx1*^{Cre} mouse line; Prof. Corinne Lobe, Sunnybrook and Women's College Health Science Centre, Toronto, Ontario, Canada, for kindly providing the Z/EG mouse line; the facilities of MPI-CBG, especially J. Helppi and the mouse facility, for excellent support; Dr Klaus Fabel, CRTD, TU Dresden, for help with some of the experiments. W.B.H. was supported by grants from the DFG (SPP 1109, Hu 275/7-3; SPP 1111, Hu 275/8-3; SFB/TR 13, B1; SFB 655, A2), by the DFG-funded Center for Regenerative Therapies, Dresden, by the Fonds der Chemischen Industrie and by the Federal Ministry of Education and Research (BMBF) in the framework of the National Genome Research Network (NGFN-2).

Supplementary material

Supplementary material for this article is available at http://dev.biologists.org/cgi/content/full/135/23/3911/DC1

References

Abdel-Mannan, O., Cheung, A. F. and Molnar, Z. (2008). Evolution of cortical neurogenesis. *Brain Res. Bull.* **75**, 398-404.

Andl, T., Murchison, E. P., Liu, F., Zhang, Y., Yunta-Gonzalez, M., Tobias, J. W., Andl, C. D., Seykora, J. T., Hannon, G. J. and Millar, S. E. (2006). The miRNA-processing enzyme dicer is essential for the morphogenesis and maintenance of hair follicles. *Curr. Biol.* **16**, 1041-1049.

Banny, T. M. and Clark, G. (1950). The new domestic cresyl echt violet. *Stain Technol.* **25**, 195-196.

Bernstein, E., Caudy, A. A., Hammond, S. M. and Hannon, G. J. (2001). Role for a bidentate ribonuclease in the initiation step of RNA interference. *Nature* **409**, 363-366.

Brinks, H., Conrad, S., Vogt, J., Oldekamp, J., Sierra, A., Deitinghoff, L., Bechmann, I., Alvarez-Bolado, G., Heimrich, B., Monnier, P. P. et al. (2004). The repulsive guidance molecule RGMa is involved in the formation of afferent connections in the dentate gyrus. *J. Neurosci.* **24**, 3862-3869.

Calegari, F., Haubensak, W., Haffner, C. and Huttner, W. B. (2005). Selective lengthening of the cell cycle in the neurogenic subpopulation of neural progenitor cells during mouse brain development. *J. Neurosci.* **25**, 6533-6538.

Cao, X., Yeo, G., Muotri, A. R., Kuwabara, T. and Gage, F. H. (2006). Noncoding RNAs in the mammalian central nervous system. *Annu. Rev. Neurosci.* **29**, 77-103.

Caviness, V. S., Jr, Takahashi, T. and Nowakowski, R. S. (1995). Numbers, time and neocortical neuronogenesis: a general developmental and evolutionary model. *Trends Neurosci.* **18**, 379-383.

Choi, P. S., Zakhary, L., Choi, W. Y., Caron, S., Alvarez-Saavedra, E., Miska, E. A., McManus, M., Harfe, B., Giraldez, A. J., Horvitz, R. H. et al. (2008). Members of the miRNA-200 family regulate olfactory neurogenesis. *Neuron* **57**, 41-55.

Conaco, C., Otto, S., Han, J. J. and Mandel, G. (2006). Reciprocal actions of REST and a microRNA promote neuronal identity. *Proc. Natl. Acad. Sci. USA* **103**, 2422-2427.

Cuellar, T. L., Davis, T. H., Nelson, P. T., Loeb, G. B., Harfe, B. D., Ullian, E. and McManus, M. T. (2008). Dicer loss in striatal neurons produces behavioral and neuroanatomical phenotypes in the absence of neurodegeneration. *Proc. Natl. Acad. Sci. USA* **105**, 5614-5619.

Davis, T. H., Cuellar, T. L., Koch, S. M., Barker, A. J., Harfe, B. D., McManus, M. T. and Ullian, E. M. (2008). Conditional loss of Dicer disrupts cellular and tissue morphogenesis in the cortex and hippocampus. *J. Neurosci.* **28**, 4322-4330.

De Pietri Tonelli, D., Calegari, F., Fei, J. F., Nomura, T., Osumi, N., Heisenberg, C. P. and Huttner, W. B. (2006). Single-cell detection of microRNAs in developing vertebrate embryos after acute administration of a dual-fluorescence reporter/sensor plasmid. *Biotechniques* **41**, 727-732.

Englund, C., Fink, A., Lau, C., Pham, D., Daza, R. A., Bulfone, A., Kowalczyk, T. and Hevner, R. F. (2005). Pax6, Tbr2, and Tbr1 are expressed sequentially by radial glia, intermediate progenitor cells, and postmitotic neurons in developing neocortex. *J. Neurosci.* **25**, 247-251.

Ferland, R. J., Cherry, T. J., Preware, P. O., Morrisey, E. E. and Walsh, C. A. (2003). Characterization of Foxp2 and Foxp1 mRNA and protein in the developing and mature brain. *J. Comp. Neurol.* **460**, 266-279.

Götz, M. and Barde, Y. A. (2005). Radial glial cells: defined and major intermediates between embryonic stem cells and CNS neurons. *Neuron* **46**, 369-372.

Götz, M. and Huttner, W. B. (2005). The cell biology of neurogenesis. *Nat. Rev. Mol. Cell Biol.* **6**, 777-788.
Hannon, G. J., Rivas, F. V., Murchison, E. P. and Steitz, J. A. (2006). The expanding universe of noncoding RNAs. *Cold Spring Harb. Symp. Quant. Biol.* **71**, 551-564.
Haubensak, W., Attardo, A., Denk, W. and Huttner, W. B. (2004). Neurons arise in the basal neuroepithelium of the early mammalian telencephalon: A major site of neurogenesis. *Proc. Natl. Acad. Sci. USA* **101**, 3196-3201.
He, X., Treacy, M. N., Simmons, D. M., Ingraham, H. A., Swanson, L. W. and Rosenfeld, M. G. (1989). Expression of a large family of POU-domain regulatory genes in mammalian brain development. *Nature* **340**, 35-41.
Hevner, R. F., Shi, L., Justice, N., Hsueh, Y., Sheng, M., Smiga, S., Bulfone, A., Goffinet, A. M., Campagnoni, A. T. and Rubenstein, J. L. (2001). Tbr1 regulates differentiation of the preplate and layer 6. *Neuron* **29**, 353-366.
Hohjoh, H. and Fukushima, T. (2007). Expression profile analysis of microRNA (miRNA) in mouse central nervous system using a new miRNA detection system that examines hybridization signals at every step of washing. *Gene* **391**, 39-44.
Hutvagner, G., McLachlan, J., Pasquinelli, A. E., Balint, E., Tuschl, T. and Zamore, P. D. (2001). A cellular function for the RNA-interference enzyme Dicer in the maturation of the let-7 small temporal RNA. *Science* **293**, 834-838.
Iwasato, T., Datwani, A., Wolf, A. M., Nishiyama, H., Taguchi, Y., Tonegawa, S., Knopfel, T., Erzurumlu, R. S. and Itohara, S. (2000). Cortex-restricted disruption of NMDAR1 impairs neuronal patterns in the barrel cortex. *Nature* **406**, 726-731.
Kim, J., Inoue, K., Ishii, J., Vanti, W. B., Voronov, S. V., Murchison, E., Hannon, G. and Abeliovich, A. (2007). A MicroRNA feedback circuit in midbrain dopamine neurons. *Science* **317**, 1220-1224.
Kloosterman, W. P., Wienholds, E., de Bruijn, E., Kauppinen, S. and Plasterk, R. H. (2006). In situ detection of miRNAs in animal embryos using LNA-modified oligonucleotide probes. *Nat. Methods* **3**, 27-29.
Kosodo, Y., Röper, K., Haubensak, W., Marzesco, A.-M., Corbeil, D. and Huttner, W. B. (2004). Asymmetric distribution of the apical plasma membrane during neurogenic divisions of mammalian neuroepithelial cells. *EMBO J.* **23**, 2314-2324.
Krichevsky, A. M., King, K. S., Donahue, C. P., Khrapko, K. and Kosik, K. S. (2003). A microRNA array reveals extensive regulation of microRNAs during brain development. *RNA* **9**, 1274-1281.
Krichevsky, A. M., Sonntag, K. C., Isacson, O. and Kosik, K. S. (2006). Specific microRNAs modulate embryonic stem cell-derived neurogenesis. *Stem Cells* **24**, 857-864.
Kriegstein, A., Noctor, S. and Martinez-Cerdeno, V. (2006). Patterns of neural stem and progenitor cell division may underlie evolutionary cortical expansion. *Nat. Rev. Neurosci.* **7**, 883-890.
Lagos-Quintana, M., Rauhut, R., Yalcin, A., Meyer, J., Lendeckel, W. and Tuschl, T. (2002). Identification of tissue-specific microRNAs from mouse. *Curr. Biol.* **12**, 735-739.
Makeyev, E. V., Zhang, J., Carrasco, M. A. and Maniatis, T. (2007). The MicroRNA miR-124 promotes neuronal differentiation by triggering brain-specific alternative pre-mRNA splicing. *Mol. Cell* **27**, 435-448.
Miska, E. A., Alvarez-Saavedra, E., Townsend, M., Yoshii, A., Sestan, N., Rakic, P., Constantine-Paton, M. and Horvitz, H. R. (2004). Microarray analysis of microRNA expression in the developing mammalian brain. *Genome Biol.* **5**, R68.
Molnar, Z., Metin, C., Stoykova, A., Tarabykin, V., Price, D. J., Francis, F., Meyer, G., Dehay, C. and Kennedy, H. (2006). Comparative aspects of cerebral cortical development. *Eur. J. Neurosci.* **23**, 921-934.
Molyneaux, B. J., Arlotta, P., Menezes, J. R. and Macklis, J. D. (2007). Neuronal subtype specification in the cerebral cortex. *Nat. Rev. Neurosci.* **8**, 427-437.
Murchison, E. P., Partridge, J. F., Tam, O. H., Cheloufi, S. and Hannon, G. J. (2005). Characterization of Dicer-deficient murine embryonic stem cells. *Proc. Natl. Acad. Sci. USA* **102**, 12135-12140.
Novak, A., Guo, C., Yang, W., Nagy, A. and Lobe, C. G. (2000). Z/EG, a double reporter mouse line that expresses enhanced green fluorescent protein upon Cre-mediated excision. *Genesis* **28**, 147-155.
Price, D. J., Kennedy, H., Dehay, C., Zhou, L., Mercier, M., Jossin, Y., Goffinet, A. M., Tissir, F., Blakey, D. and Molnar, Z. (2006). The development of cortical connections. *Eur. J. Neurosci.* **23**, 910-920.
Rakic, P. (1995). A small step for the cell, a giant leap for mankind: a hypothesis of neocortical expansion during evolution. *Trends Neurosci.* **18**, 383-388.
Rakic, P. (2007). The radial edifice of cortical architecture: from neuronal silhouettes to genetic engineering. *Brain Res. Rev.* **55**, 204-219.
Schaefer, A., O'Carroll, D., Tan, C. L., Hillman, D., Sugimori, M., Llinas, R. and Greengard, P. (2007). Cerebellar neurodegeneration in the absence of microRNAs. *J. Exp. Med.* **204**, 1553-1558.
Sempere, L. F., Freemantle, S., Pitha-Rowe, I., Moss, E., Dmitrovsky, E. and Ambros, V. (2004). Expression profiling of mammalian microRNAs uncovers a subset of brain-expressed microRNAs with possible roles in murine and human neuronal differentiation. *Genome Biol.* **5**, R13.
Shcherbata, H. R., Ward, E. J., Fischer, K. A., Yu, J. Y., Reynolds, S. H., Chen, C. H., Xu, P., Hay, B. A. and Ruohola-Baker, H. (2007). Stage-specific differences in the requirements for germline stem cell maintenance in the Drosophila ovary. *Cell Stem Cell* **1**, 698-709.
Simeone, A., Gulisano, M., Acampora, D., Stornaiuolo, A., Rambaldi, M. and Boncinelli, E. (1992). Two vertebrate homeobox genes related to the Drosophila empty spiracles gene are expressed in the embryonic cerebral cortex. *EMBO J.* **11**, 2541-2550.
Smirnova, L., Grafe, A., Seiler, A., Schumacher, S., Nitsch, R. and Wulczyn, F. G. (2005). Regulation of miRNA expression during neural cell specification. *Eur. J. Neurosci.* **21**, 1469-1477.
Stark, A., Brennecke, J., Bushati, N., Russell, R. B. and Cohen, S. M. (2005). Animal MicroRNAs confer robustness to gene expression and have a significant impact on 3'UTR evolution. *Cell* **123**, 1133-1146.
Stefani, G. and Slack, F. J. (2008). Small non-coding RNAs in animal development. *Nat. Rev. Mol. Cell Biol.* **9**, 219-230.
Watanabe, T., Totoki, Y., Toyoda, A., Kaneda, M., Kuramochi-Miyagawa, S., Obata, Y., Chiba, H., Kohara, Y., Kono, T., Nakano, T. et al. (2008). Endogenous siRNAs from naturally formed dsRNAs regulate transcripts in mouse oocytes. *Nature* **453**, 539-543.
Wonders, C. P. and Anderson, S. A. (2006). The origin and specification of cortical interneurons. *Nat. Rev. Neurosci.* **7**, 687-696.
Wu, L. and Belasco, J. G. (2005). Micro-RNA regulation of the mammalian lin-28 gene during neuronal differentiation of embryonal carcinoma cells. *Mol. Cell. Biol.* **25**, 9198-9208.